FATIGUE ANALYSIS OF A WELDED HUB FOR A MID POWER WIND TURBINE

P. Goes[a], F. Van den Abeele[a], X. Vanwijck[b], A. De Broe[b], H. Ahmed[a],

[a] OCAS N.V., Zelzate, Belgium
[b] 3E, Brussels, Belgium

Abstract The hub of a mid-power wind turbine can be made directly from a mould (cast iron), or by welding the three blade connections onto the main body. From a structural point of view, a cast hub is more efficient to withstand fatigue loading, but from a manufacturing (and economic) point of view, a welded solution is preferred.

In this paper, a lifetime analysis is presented to predict the accumulated fatigue damage of a welded hub under different operating conditions. The fatigue analysis covers normal operation, start-up, normal shutdown and parked conditions. In addition, the effects of faults like overspeed, maximum yaw error and grid failure are taken into account in the lifetime estimation.

A finite element model is implemented, with load time histories for the forces {Fx, Fy, Fz} and moments {Mx, My, Mz}. In the fatigue analysis, rainflow counting is performed to reduce the number of calculations, and hot spot detection is used to identify the most critical zone. The results of the fatigue analysis indicate the severity of the different load cases, and confine the design space for lifetime optimization.

Keywords Fatigue analysis, welded hub, wind turbine, rainflow counting, hot spots

1 INTRODUCTION

In the distributed wind energy industry, it is widely noted that one of the largest impediments to the industry's growth is a lack of available turbines in the range of 50 kW to 500 kW [01]. In order to bridge this gap in the wind energy market, 3E –a Belgian company based in Brussels- is currently developing a medium size wind turbine for off-grid and distributed generation applications: the XANT-21 wind turbine. Especially the off-grid market segment (wind-diesel systems) requires extremely reliable turbines that can be installed without heavy equipment. In a first feasibility study, the technical requirements of the complete wind turbine were examined and new concepts for aerodynamics, electromagnetics and mechanical design were reviewed. Throughout the product development cycle, selected concepts are integrated in a certified wind turbine design. Prototyping will start at the end of 2011.

Mainframe design	**Initial hub design**
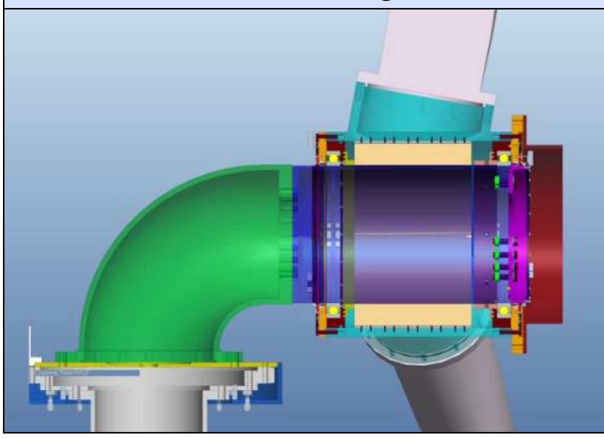	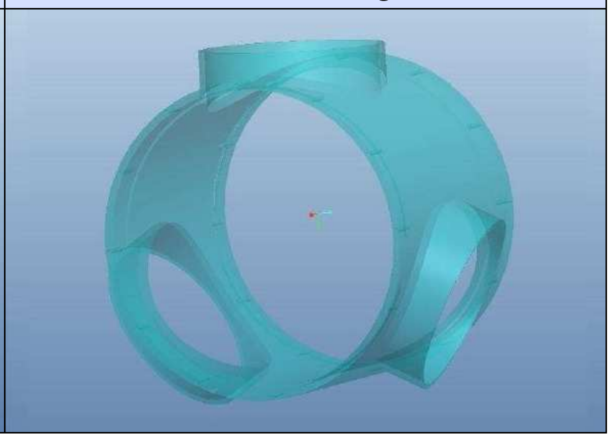

Figure 1: Initial concept design of the mainframe and the hub

The hub of such a mid-power wind turbine can be made directly from a mould (cast iron), or by welding the three blade connections onto the main body. From a structural point of view, a cast hub is more efficient to withstand fatigue loading, but from a manufacturing (and economic) point of view, a welded solution may be better. In addition, large components with thin walls cannot be cast due to viscosity issues.

Like shown on Figure 1, the hub consists of a main body (i.e. a section of standard steel pipe) and three blade connections (where each connection corresponds to another section of standard steel pipe). As cost and simplicity are the main design drivers for the whole mid-power wind turbine, a welded solution is desired for the hub, provided that the structure (and in particular the welds) can withstand the anticipated fatigue loads during the entire design life (20 years) of the wind turbine.

In this paper, a fatigue analysis for the welded hub is presented. In the welded hub, fatigue initiation is assumed to have occurred in the welds (e.g. due to lack of fusion, poor penetration or weld porosity). In addition, the shape of the weld bead acts as a stress raiser, promoting fatigue crack growth. A solid finite element model is implemented to accurately capture the stress concentrations that may give rise to fatigue failure. The results of the numerical simulations with solid elements are combined with the load time histories for forces and moments to calculate fatigue damage accumulation during normal operation, start-up, shut-down, under parked conditions and in the occurrence of a fault (like over-speed, yaw error and grid failure).

2 PREDICTION OF STRESS CONCENTRATIONS

The optimized design of the welded hub is used for static stiffness and strength calculations, enabling the prediction of stress concentrations or ‘hot spots’ like sharp changes in section, surface discontinuities, porosity, weld beads,... For the elastic properties of the steel, a Young’s modulus E = 210 000 MPa and a Poisson contraction coefficient $\nu = 0.3$ is used, with a steel density $\rho = 7850$ kg/m³. The main body is assumed perfectly plastic, with a yield stress $\sigma y = 355$ MPa. For the inserts, the same material model is applied, although a parametric formulation allows easy modifications and comparison of different material combinations. For the weld seam, an overmatching weld metal ($\sigma_y = 500$ MPa) with a thickness of 10 mm is chosen.

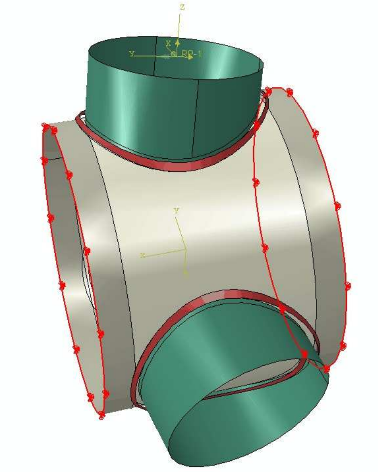

Figure 2: Boundary conditions for the finite element model

The boundary conditions for the finite element model are schematically shown on Figure 2. The displacement degrees of freedom are constrained at both ends of the hub, and a local coordinate system is introduced at the blade root to define the load components. The loads acting from the hub are exercised by the blades, through the blade connections. The maximum expected loads, transformed to the coordinate system of Figure 2, are listed in Table 1:

Table 1: Maximum expected loads acting on the hub

Load	Value	Unit	Origin
F_x	2.5	kN	Blade weight
F_y	6	kN	Aerodynamic load
F_z	38	kN	Centrifugal force
M_x	86	kNm	Flapwise aerodynamic load
M_y	14	kNm	Weight and sudden brake
Mz	0	kNm	Torsion

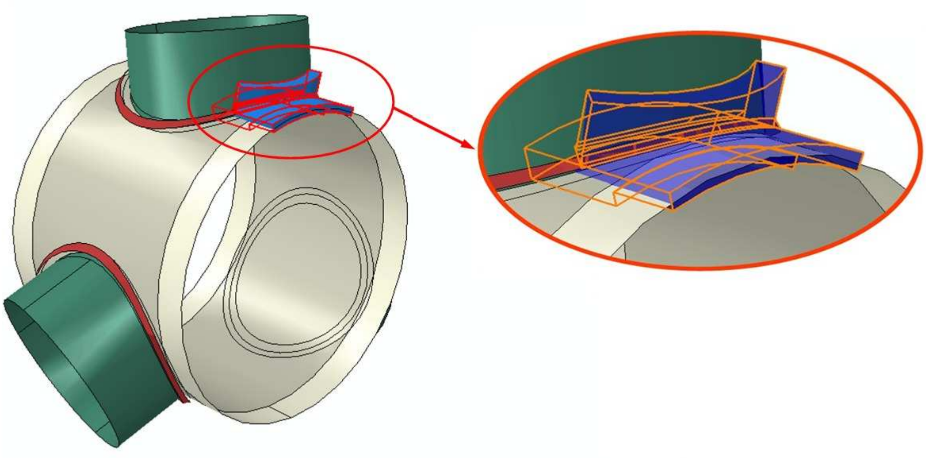

Figure 3: Critical zone for stress concentrations

Like shown on Figure 3, the most critical zone is the part of the main hub body where the wall thickness is reduced to accommodate the bearing. The stress concentrations in this zone may give rise to fatigue failure under cyclic loading. In order to accurately capture the stresses in this critical zone, an increased mesh density is applied in this area, like shown on Figure 4. In total, 656 052 tetrahedral elements are used, resulting in a problem size of 387 804 degrees of freedom.

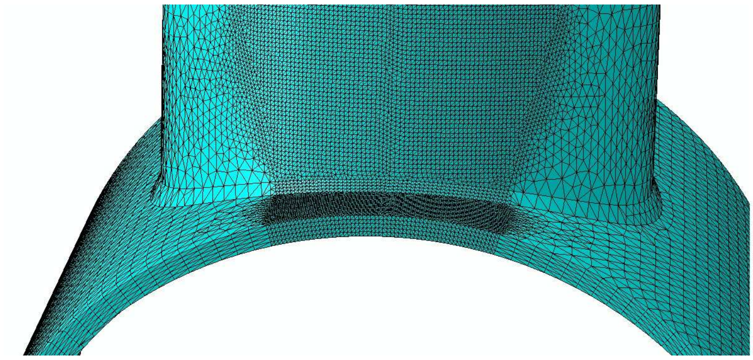

Figure 4: Mesh detail in the vicinity of the critical zone

The Von Mises stress distribution in the welded hub subjected to combined loading is shown on Figure 5. The equivalent stress at the inner surface of the bearing housing is σ_{eqv} = 55 MPa, and the maximum stress σ_{max} = 65 MPa occurs in the vicinity of the outer weld bead. Hence, this is the most critical zone for the fatigue analysis. Indeed, in a welded component, fatigue initiation is assumed to have occurred in the welds (e.g. due to lack of fusion, poor penetration or weld porosity). In addition, the shape of the weld bead acts as a stress raiser, promoting fatigue crack growth. As a result, the weld at the outside of the connection between the main hub body and the blade inserts is most susceptible to fatigue failure.

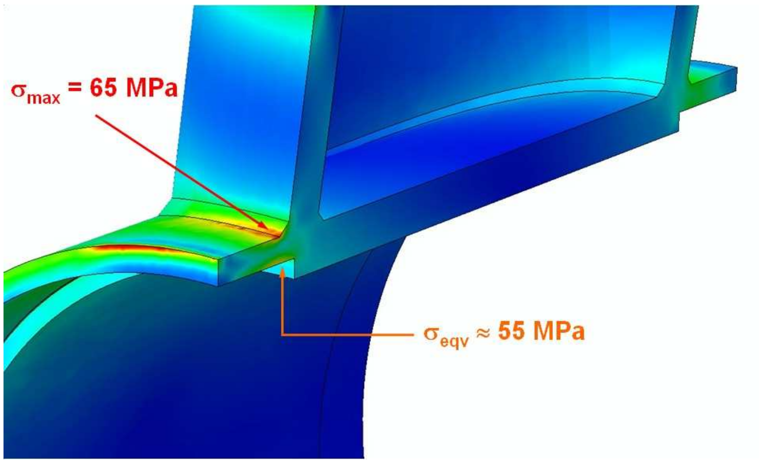

Figure 5: Von Mises stress distribution in a cross section of the hub

3 FATIGUE ANALYSIS OF THE WELDED HUB

The fatigue analysis of the welded hub is performed using the solid finite element model, introduced in the previous section, combined with the load time histories for forces $\{F_x, F_y, F_z\}$ and moments $\{M_x, M_y, M_z\}$, like shown on Figure 6.

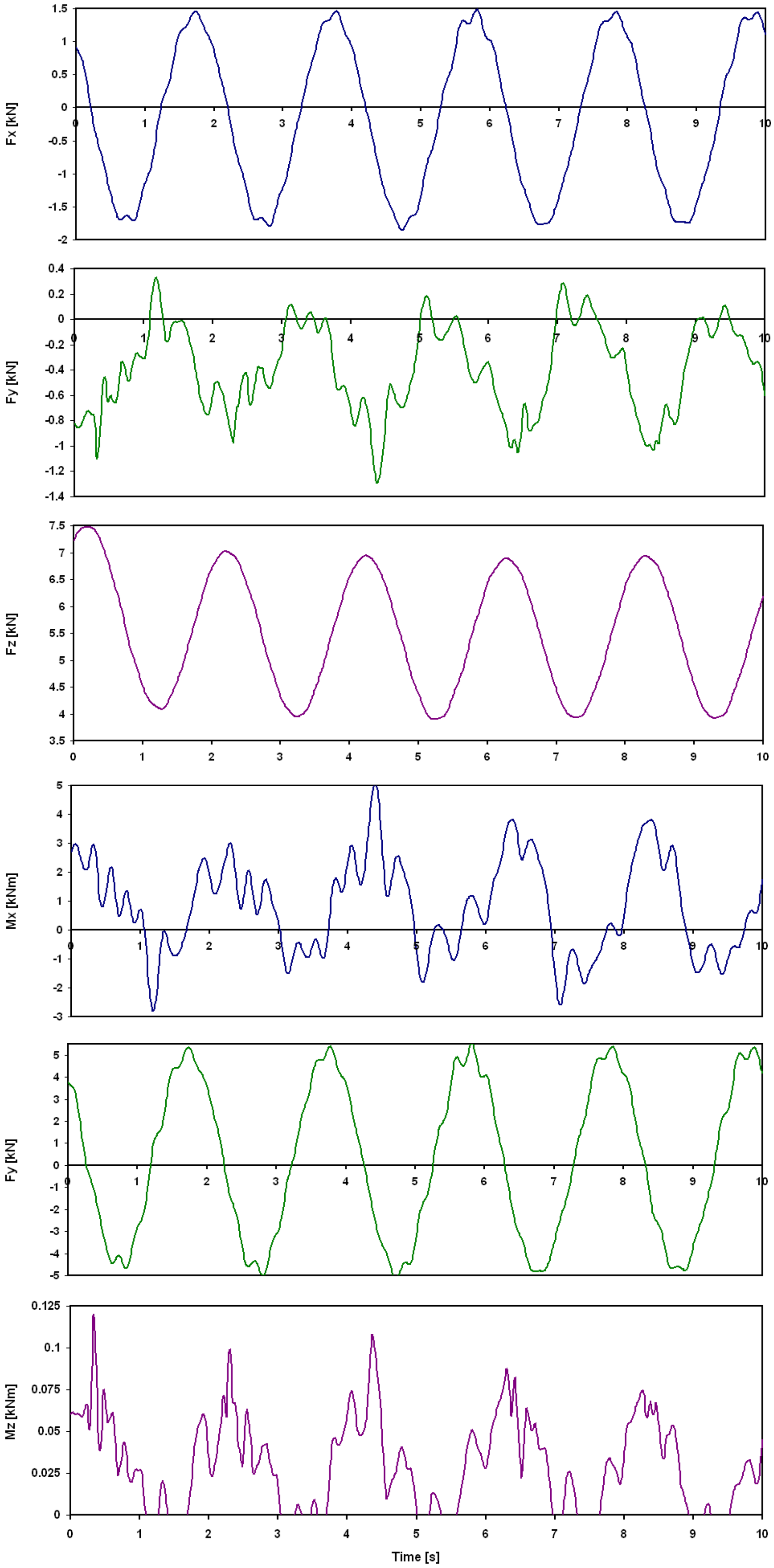

Figure 6: Excerpt of the time series for forces and moments acting on a windmill blade

The procedure follows the IEC guideline (Annex G – Fatigue Analysis) using Miner's rule with load extrapolation. This rule states that if the six different load cases S_i each contribute n_i cycles, failure occurs when

$$\sum_{i=1}^{6} \frac{n_i}{N_i} = 1 \qquad \text{(Eq. 01)}$$

where N_i is the number of cycles to failure of a constant stress reversal Si. Expression (Eq. 01) can be read as evaluating which proportion of life is consumed by stress reversal at each magnitude, and subsequently constructing a linear combination of their aggregate.

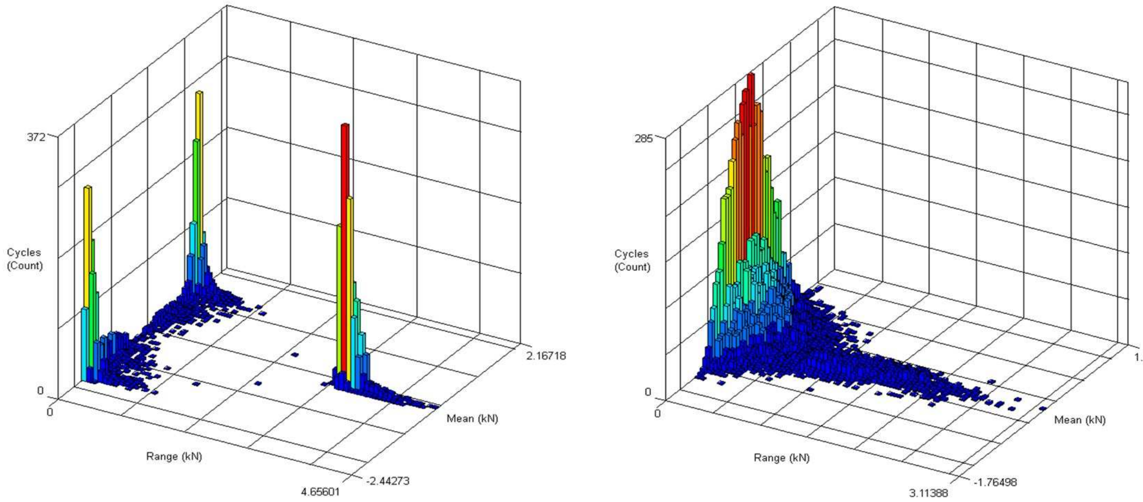

Figure 7: Rainflow count histogram for fatigue analysis of multiple stress cycles

The effects of the maxima and minima of the stress series are identified using the rain-flow cycle counting: instead of calculating the fatigue damage for each individual cycle, the damage for each bin of histograms (shown on Figure 7) is calculated, and multiplied by the number of cycles in that bin.

The considered wind speed follows a Rayleigh distribution [02]

$$f\left(v|\sigma\right) = \frac{v}{\sigma^2} \exp\left[-\frac{1}{2}\left(\frac{v}{\sigma}\right)^2 \right] \qquad \text{(Eq. 02)}$$

which is a special case of the Weibull function

$$f\left(v|\lambda,k\right) = \frac{k}{\lambda}\left(\frac{v}{\lambda}\right)^{k-1} \exp\left[-\left(\frac{v}{\lambda}\right)^k \right] \qquad \text{(Eq. 03)}$$

for k = 2 and $\sigma = \lambda/\sqrt{2}$. On Figure 8, both (Eq. 03) and the cumulative probability density function

$$F\left(v|\sigma\right) = 1 - \exp\left[-\frac{1}{2}\left(\frac{v}{\sigma}\right)^2 \right] \qquad \text{(Eq. 04)}$$

are shown. The partial safety factors for loads is γ = 1.0 for all normal and abnormal design situations. For welded and structural steel, the considered S/N curve is based on a 97.7% survival probability. Hence, according to [02], the material safety factor is chosen as γ_m = 1.1. Safety factors for consequences of failure are listed in Table 2.

Table 2: Satefy factors for consequences of failure

Component class	Safety factor
1	1.0
2	1.15
3	1.30

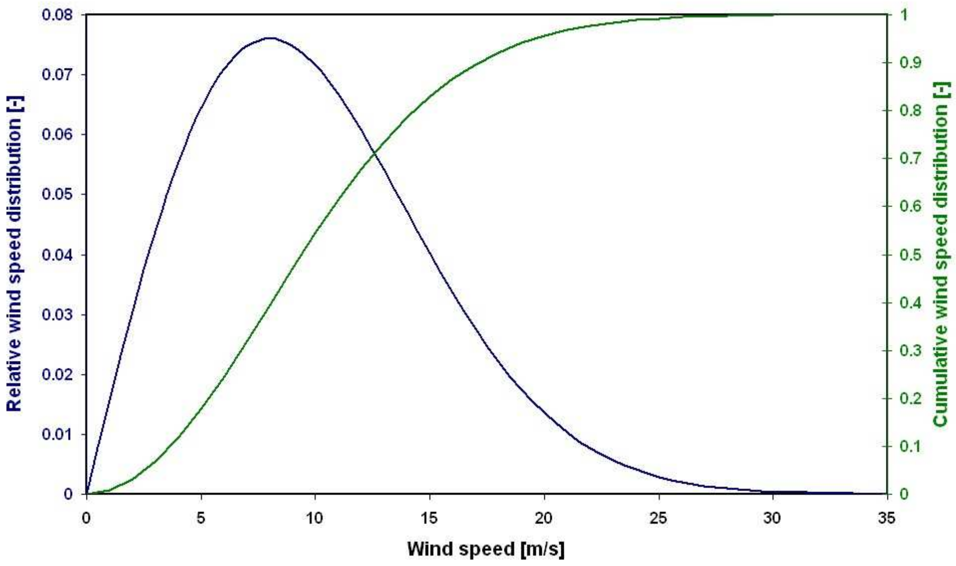

Figure 8: Relative and cumulative Rayleigh probability functions of wind speed distribution

The design S/N curves used for the damage calculation of the steel parts of the wind turbine (in particular the welded hub) are taken from [03]. The geometry of the weld determines the weld fatigue class, which governs the Wöhler curve of stress range S versus cycles N. In the analysis presented here, a steel weld BS5400 Class F2 is chosen, with the corresponding S/N curve of Figure 9.

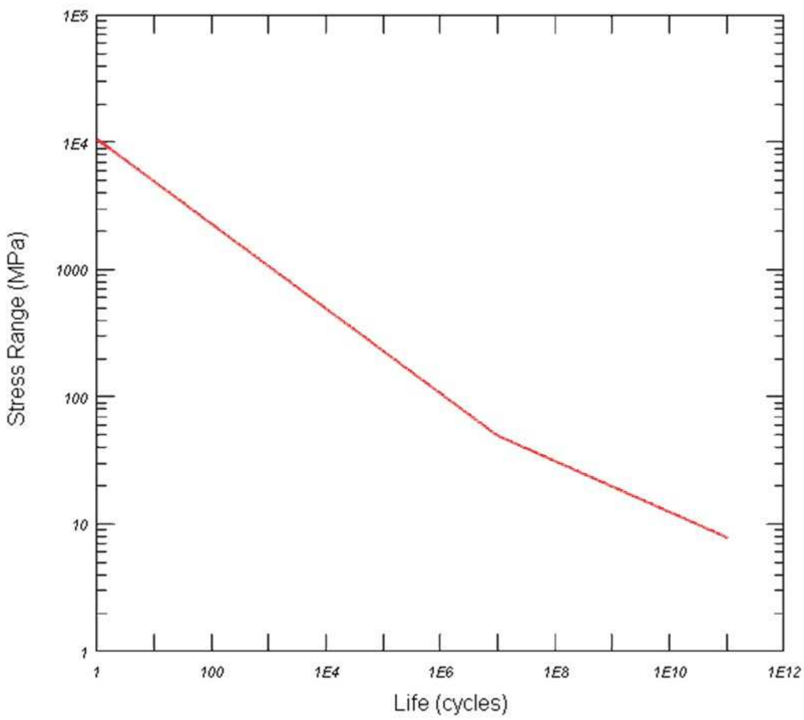

Figure 9: Wöhler curve for steel weld BS5400 Class F2

According to [02], the fatigue analysis concerns the following load cases:

- DLC 1.2 Normal operation
- DLC 2.4 Normal operation + occurrence of fault
- DLC 3.1 Start-up
- DLC 4.1 Normal shutdown
- DLC 6.3 Parked

Table 3: Occurrence of the design load cases

Load case	Design situation	Occurrence [%]
DLC 1.2	Normal operation	86.51
DLC 2.4	Normal operation + occurrence of fault	0.14
DLC 3.1	Start-up	0.70
DLC 4.1	Normal shutdown	0.70
DLC 6.4	Parked	11.95
Total		**100**

The DLC 1.2 and DLC 6.3 are directly connected to the wind distribution, and therefore linked to the site. For this fatigue load assumption, a class IA site is considered. The number of occurrences for DLC 3.1 and DLC 4.1 is indicated in [04]. The faults (DLC 2.4) can occur at *any* wind speed. The repartition of the load cases during the design life time of the wind turbine is given in Table 3.

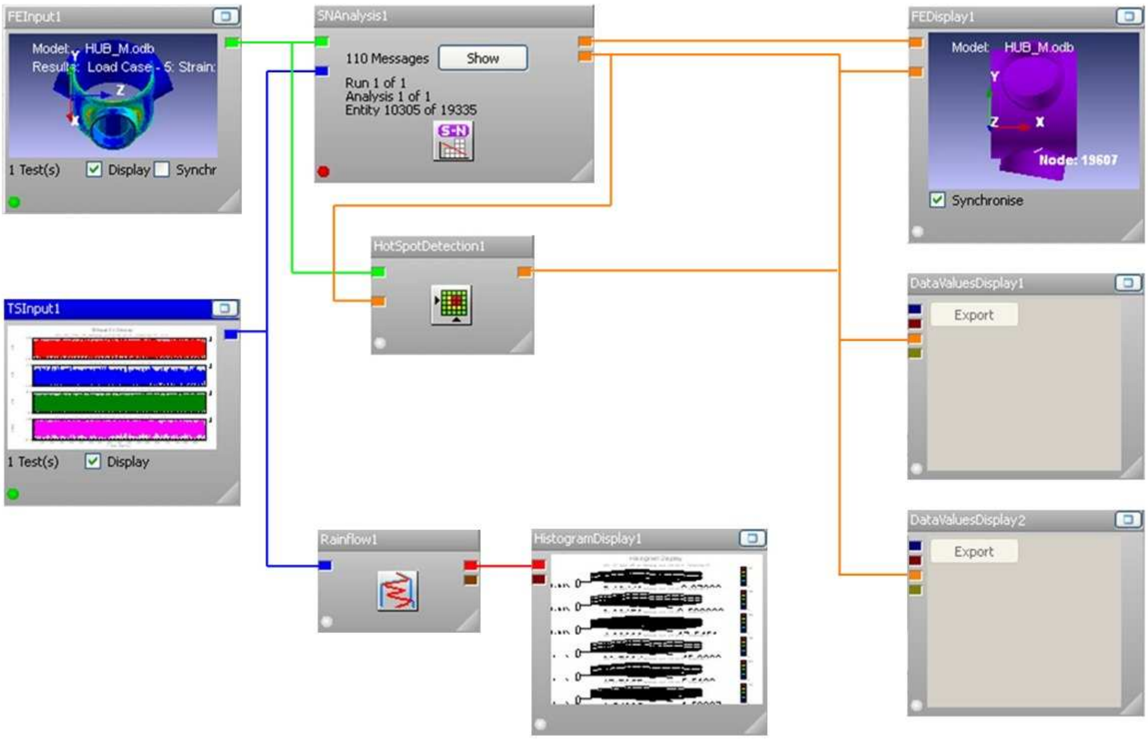

Figure 10: Flowchart for fatigue failure calculations

The flowchart for the fatigue failure calculations is schematically shown on Figure 10. The solid finite element model with unit loads (F = 1 kNm for forces, M = 1 kNmm for moments) is used as an input. The signals of the time series $\{F_x, F_y, F_z, M_x, M_y, M_z\}$ are used to scale the amplitudes of the FEA load cases. In the fatigue analysis, a rainflow counting is performed to reduce the number of calculations. For each bin, the fatigue damage is calculated based on the S/N curve, and multiplied by the number of cycles in that bin. Hot spot detection is used to identify the most critical zone. The predicted fatigue failure is displayed, and combined with the information of the hot spot detection tool. The fatigue damage and the location of the hot spots are exported as data files.

3.1 Fatigue damage induced by normal operation

Between cut-in and cut-out wind speeds, a Rayleigh distribution for a class IA site is taken into account to determine the weight of each bin. On Figure 11, the results of a finite element analysis for an unscaled component of force and moment are shown, indicating that the stress concentrations depend on the load case considered.

Force	Moment
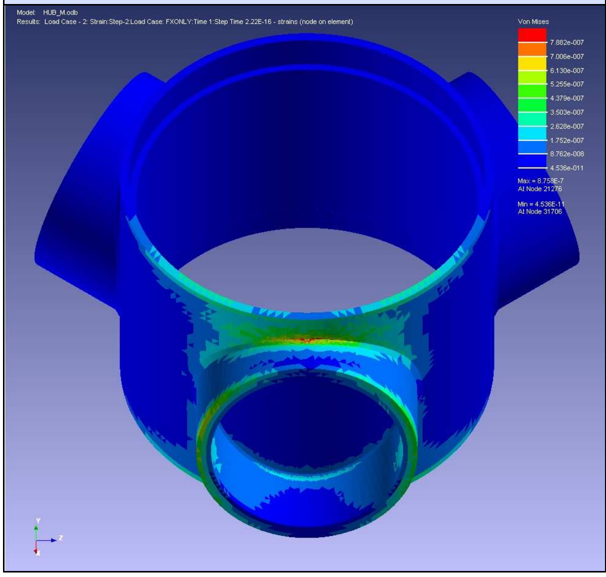	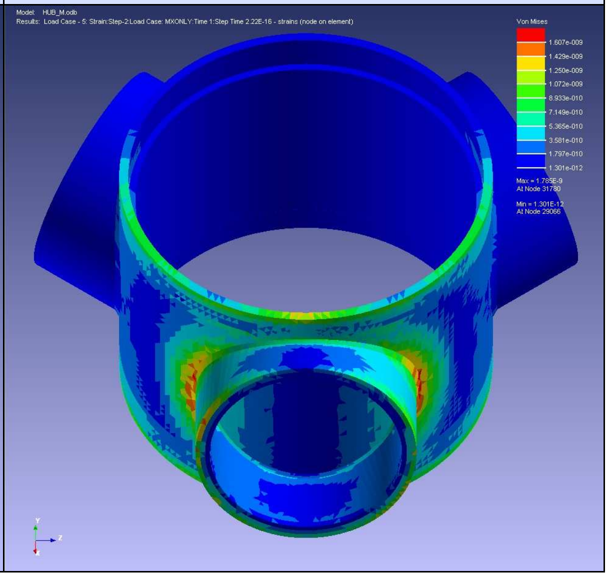

Figure 11: Finite element analysis results for different load cases

For every time series, the fatigue damage Ds is determined by the fatigue analysis, like shown on Figure 12. Subsequently, the damage per second can be calculated as

$$D_f^s = \frac{D_f}{\Delta T} \qquad \text{(Eq. 05)}$$

with ΔT the length of the time series. The expected damage during the entire design life (20 years) is then obtained as

$$D_f^L = D_f^s \, N_s \qquad \text{(Eq. 06)}$$

with Ns the total number of seconds that the hub is in this state, based on the Rayleigh distribution of the wind speed. Figure 13 shows the damage per second as a function of wind speed for normal operation.

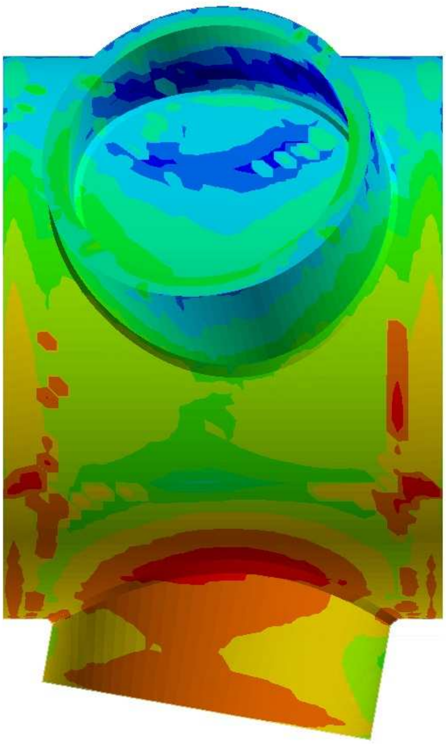

Figure 12: Predicted fatigue damage for one time series during normal operation

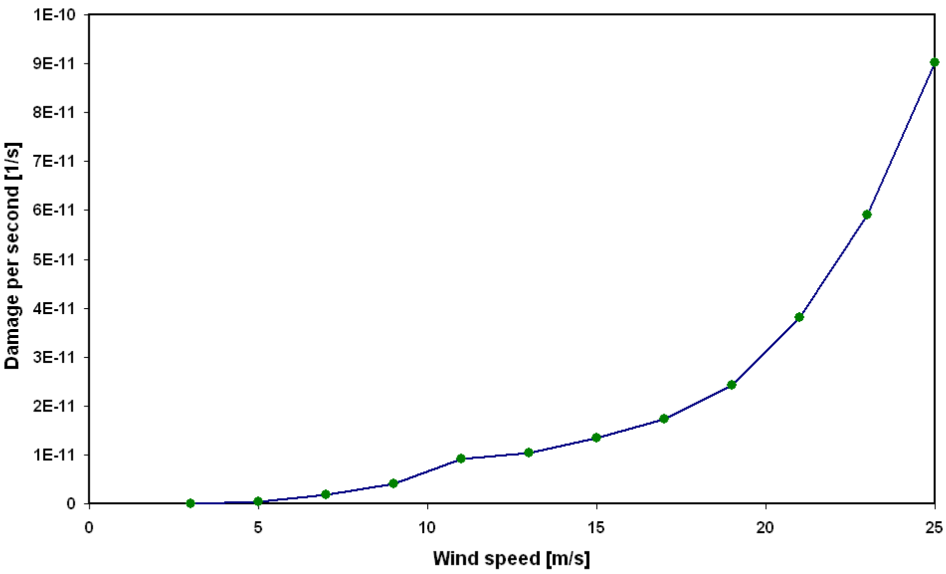

Figure 13: Fatigue damage per second as a function of wind speed for normal operation

The total fatigue damage for each time series is found by adding the damage variables for every time series within the design load case:

$$D_{tot} = \sum_{j=1}^{N} \left(D_f^L \right)_j \qquad \text{(Eq. 07)}$$

The total fatigue damage is finally found by adding the damage variables for every time series within the design load case. The total fatigue damage, induced by normal operation over a design life of 20 years, is found to be **D_{tot} = 4.72 E-2**. Hence, the current design has a safety factor of 212.

3.2 Fatigue damage induced by parked condition

The wind turbine is parked (Design Load Case DLC 6.3) if the velocity of the hub is either lower than V_{in} or higher than V_{out} , or during grid outage. The first two conditions on V_{hub} are driven by a Rayleigh distribution for a class IA site. Below the cut-in wind speed, the turbine is idling. Above the cut-out wind speed and during grid outages, the wind turbine is shut down using an electrical brake.

Overall grid availability in developing countries is ± 95%, implying 1.2 hours of outage per day. Measurements show 4-5 outages in a 200 hours period [04], but these measurements were at 110 kV level. Hence, the number of grid interruptions at the wind turbine terminals is expected to be higher. Again, the distribution of the wind during these outages is assumed to follow a Rayleigh distribution of class IA site.

The analysis to calculate the total fatigue damage induced by the parked condition during the anticipated design life of the wind turbine follows the same flowchart as shown on Figure 10, and was explained in the previous section. The total damage is found to be **D_{tot} = 7.45 E-4**, which is even six times smaller than the fatigue damage for normal operation.

3.3 Fatigue damage induced during start-up

The occurrences of start-up (Design Load Case DLC 3.1) follow [04], with 1000 start-up procedures per year at V_{in}, 50 at V_r and 50 at V_{out}. The time series for the same wind conditions are concatenated into a single series. In this case, only three wind directions (0° and ± 8°) are considered for each wind speed. The fatigue analysis reveals that the total damage induced by start-up procedures (**Dtot = 7.44 E-8**) can be neglected.

3.4 Fatigue damage induced during normal shutdown

The occurrences of normal shut-down (Design Load Case DLC 4.1) follow [04], with 1000 stopping procedures per year at V_{in}, 50 at V_r and 50 at V_{out}. The fatigue analysis yields a total damage induced by shutdown procedures **of D_{tot} = 7.87 E-9**, which is ten times smaller than the (negligible) fatigue damage during start-up.

3.5 Occurrence of a fault

Three faults are considered for the fatigue analysis of Design Load Case DLC 2.4: over-speed, maximum yaw error and grid failure:

- For **over-speed**, [04] is followed, which specifies 10 shutdowns per year due to first over-speed. The results from DLC 2.1 are used for the fatigue analysis. Four wind speeds are considered (9, 11, 13 and 25 m/s), with an equal probability of occurrence.
- For **maximum yaw error**, the considered yaw error is 90° within an occurrence of 24 hours per year, according to [04]. Once again, the results from DLC 2.1 are used for the same four wind speeds, with an equal probability of occurrence.
- For **grid failure**, the worst case scenario of one grid failure per day [05] is assumed.

The total fatigue damage due to faults is found to be very small, i.e. $\mathbf{D_{tot} = 1.30\ E\text{-}6}$.

3.6 Summary of the fatigue analysis

The results of the fatigue analysis are summarized in Table 4, showing that normal operation is the most important (and most severe) load case. However, the total fatigue damage over the anticipated lifetime is still very small. The current design has a safety factor higher than 200, which provides ample opportunity for thickness reduction.

Table 4: Total fatigue damage for the different design load cases

Load case	Design situation	Occurrence [%]	Damage [-]
DLC 1.2	Normal operation	86.51	4.72 E-3
DLC 6.4	Parked	11.95	7.45 E-4
DLC 3.1	Start-up	0.70	7.44 E-8
DLC 4.1	Normal shutdown	0.70	7.87 E-9
DLC 2.4	Normal operation + occurrence of fault	0.14	1.30 E-6

4 CONCLUSIONS

In this paper, a fatigue lifetime analysis was presented to predict the accumulated fatigue damage during normal operation, start-up, shut-down, under parked conditions and in the occurrence of a fault (like over-speed, yaw error or grid failure). The fatigue analysis indicates that normal operation is by far the most important design load case, and that the current design has a safety factor of more than 200, which provides ample opportunity for weight and thickness reduction and thus (in)direct cost savings.

5 REFERENCES

[01] R. Kwartin, A. Wolfrum, K. Granfield, A. Kagel and A. Appleton, *An Analysis of the Technical and Economic Potential for Mid Scale Distributed Wind*, National Renewable Energy Laboratory, report NREL/SR-500-44280 (2008)

[02] IEC 61400 – 1:2005 (Edition 3) Part 1: *Wind Turbine Design Requirements* (2005)

[03] Eurocode 3: Design of Steel Structures, Part 1.9: Fatigue

[04] Germanischer Lloyd, *Guideline for the Certification of Wind Turbines*, Edition 2003 with Supplement 2004

[05] P. Sorensen, A.K. Unnikrishan and A. M. Sajan, *Wind Farms Connected to Weak Grids in India*, Riso National Laobratory, Wind Energy 2001, vol. 4, pp. 137-149 (DOI: 10.1002/we.52)